Geophys. J. Int. (1995) **122,** 97–107

Pedogenic and lithogenic contributions to the magnetic susceptibility record of the Chinese loess/palaeosol sequence

Pinchas Fine,[1] Kenneth L. Verosub[2] and Michael J. Singer[3]

[1]*Institute of Soils and Water, ARO, The Volcani Center, Bet Dagan* 50250, *Israel*
[2]*Department of Geology, University of California, Davis,* CA 95616, *USA*
[3]*Department of Land, Air and Water Resources, University of California, Davis,* CA 95616, *USA*

Accepted 1994 December 13. Received 1994 October 25; in original form 1994 February 4

SUMMARY

We have studied the magnetic properties of 69 loess and palaeosol samples from the loess plateau in China. Our methodology involves the combination of differential dissolution of secondary iron oxides and oxyhydroxides using citrate-bicarbonate-dithionite (CBD) with measurements of magnetic parameters. Because most of these parameters are additive, we can use pre- and post-CBD values to determine the mineral magnetic properties of the CBD-soluble material. We can also calculate the partitioning of iron among various phases. Approximately two-thirds of the total iron in our samples exists as paramagnetic iron in silicate minerals. Antiferromagnetic material (haematite) constitutes almost all of the remainder. However, the magnetic susceptibility record of the loess/palaeosol sequence arises primarily from a small amount of iron in ferrimagnetic phases. This iron consists of a CBD-resistant component which represents multidomain grains inherited from the parent material of the loess, and a CBD-soluble component which represents grains near the superparamagnetic/single domain boundary. The first component appears in nearly uniform amounts throughout the loess column and is the dominant ferrimagnetic phase in the magnetically less-enhanced loess. Accumulation of the second component in the palaeosols gives rise to the magnetic susceptibility enhancement of the loess column. The magnetic properties of the CBD-soluble component indicate that it formed as a result of *in situ* pedogenesis, which confirms our earlier conclusion that the palaeoclimate record of the loess/palaeosol sequence at the sites that we have sampled is primarily a record of pedogenesis.

Key words: CBD, iron transformations, loess, magnetic mineralogy, magnetic susceptibility, palaeoclimate, palaeosols, pedogenesis.

1 INTRODUCTION

The Chinese loess plateau consists of less-weathered loess interstratified with more highly weathered palaeosols. This interstratification is evidence for significant and cyclic climatic fluctuations. The palaeosols have higher values of low-field mass magnetic susceptibility than the loess, and variations in magnetic susceptibility correlate well with the oxygen isotope record of the deep sea (Heller & Liu 1986; Kukla *et al.* 1988). Thus, the magnetic susceptibility record of the loess/palaeosol sequence is considered an excellent proxy for the quantitative study of terrestrial climatic fluctuations during the past 2.4 million years (Heller & Liu 1986).

1.1 Mechanisms of magnetic susceptibility enhancement

Initially, the enhancement of the magnetic susceptibility of the loess column in China was attributed to a constant cosmic influx of ferrimagnetic material mixed with varying amounts of non-magnetic loess (Kukla *et al.* 1988; Kukla & An 1989). It was also suggested that post-depositional processes in the soil profile might modify the magnetic susceptibility signal (Heller & Liu 1984). At the present time, *in situ* pedogenic formation of ferrimagnetic material is favoured as the mechanism of the enhancement. This view became widely accepted when several studies showed that the mineral magnetic properties of the palaeosols are significantly different from those of the loess, indicating that

post-depositional transformations have taken place (Zhou *et al.* 1990; Zheng *et al.* 1991; Heller *et al.* 1991; Maher & Thompson 1991, 1992; Liu *et al.* 1992; Hus & Han 1992; Fine, Singer & Verosub 1993; Verosub *et al.* 1993).

One important measure of the extent of pedogenesis is the concentration of pedogenic secondary iron oxides and oxyhydroxides (secondary FeOX) (e.g. Rebertus & Buol 1985) that result from the weathering of primary iron-bearing minerals. A citrate-bicarbonate-dithionite (CBD) treatment procedure (Mehra & Jackson 1960) has recently been shown to be effective in selectively dissolving the secondary FeOX while leaving behind the unweathered iron-bearing grains (Singer *et al.* 1995; Hunt *et al.* 1995). The latter are mostly paramagnetic iron in silicate minerals (Mehra & Jackson 1960) and smaller proportions of primary or lithogenic iron oxides (e.g. magnetite and titanomagnetites) inherited from the parent material (Walker 1983; Fine & Singer 1989; Singer *et al.* 1995).

In this paper, we have combined various mineral magnetic measurements with the CBD extraction procedure to determine the distribution, properties, and origin of the iron minerals in general, and the ferrimagnetic phases in particular, in the Chinese loess column. Our specific objectives are to determine the role of pedogenesis in the enhancement of the magnetic susceptibility and to compare the transformations that have occurred among the various magnetic phases in the loess and the palaeosols.

2 SAMPLES AND EXPERIMENTAL PROCEDURES

2.1 Loess and palaeosol samples

Our study is based on 44 palaeosol samples and 21 loess samples provided for us by George Kukla of the Lamont–Doherty Earth Observatory and by Barbara Maher of the University of East Anglia. Slightly less than two-thirds of the samples were collected near Luochuan, while the remainder were collected near Liujiapo in the Peoples' Republic of China (Fig. 1). The samples extend from zero depth (modern soil) to 168 m below the present land surface and encompass four of the six major units of the loess/palaeosol sequence, as described by Kukla & An (1989). From top to bottom, the six units are the Holocene Black Loam, the Malan Loess, the Upper Lishi Formation, the Lower Lishi Formation, the Wucheng Formation, and the basal Red Clay. Only the Black Loam and the Red Clay are not represented in our samples. Five pairs of samples that represent couplets of a palaeosol and its underlying loess, designated for example as S8/L9, were studied more comprehensively.

2.2 Magnetic and chemical procedures

For each sample we measured a variety of mineral magnetic properties before and after CBD treatment. This treatment involved dissolution of iron with a strong reducing agent (dithionite) and then chelation and stabilization (citrate) in a buffered solution (bicarbonate) (Singer & Janitzky 1986). The amount of CBD-soluble iron was designated as Fe_d. Using carefully sized grains of synthetic magnetite and maghemite, Hunt *et al.* (1995) recently showed that the CBD treatment dissolves maghemite grains of all sizes, maghemite rims on large magnetite grains and magnetite grains smaller than about one micron. Because these three species are the most likely ferrimagnetic phases resulting from pedogenesis, it is appropriate to use the term 'pedogenic' to describe whatever the CBD process removes from samples of the loess–palaeosol sequence.

Magnetic susceptibility, remanence and coercivity parameters were measured on samples packed in 6.5 ml plastic boxes and secured with rubber foam. The amount of soil used for each magnetic measurement was ≈4 g. After CBD treatment, the soil residue was dried at 60 °C and saved for magnetic measurements. Changes in magnetic properties resulting from the CBD treatment were determined from measurements made on the same sample. The total iron concentration (Fe_t) was determined with an inductively coupled plasma spectrometer after dissolution of samples in hydrofluoric acid.

Magnetic susceptibility (χ) was measured with a Bartington MS2 meter and MS2B sensor at frequencies of

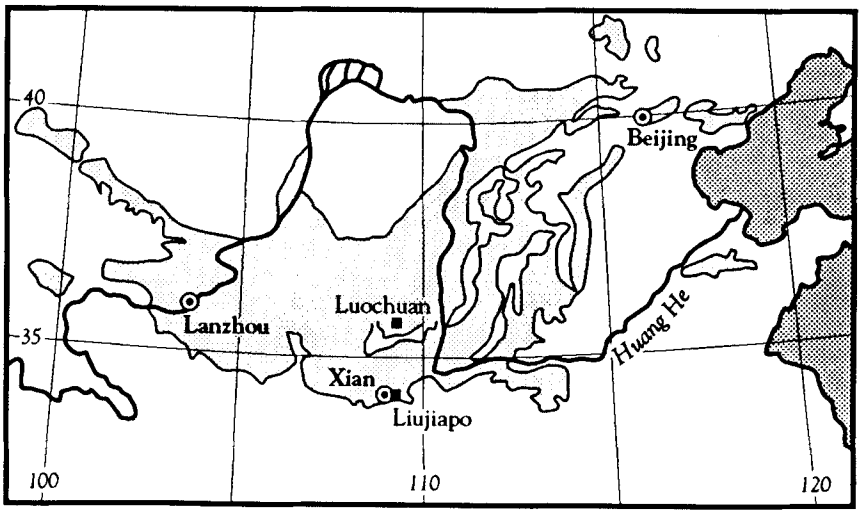

Figure 1. Map showing locations of sampling sites and main cities on the loess plateau in China.

0.47 and 4.7 kHz. The frequency dependence of the magnetic susceptibility (χ_{FD}) was calculated from the difference in the magnetic susceptibility at the two frequencies divided by the low-frequency susceptibility. This value is reported as a percentage. Anhysteretic remanent magnetization (ARM) and isothermal remanent magnetization (IRM) were acquired after three-axis demagnetization in a 99.9 mT alternating field.

ARM was acquired with a 0.150 mT direct current (dc) field in the presence of a 99.9 mT alternating field. Anhysteretic susceptibility (χ_{ARM}) was calculated from the induced ARM and the applied dc field. IRM was acquired by subjecting samples to a high-field electromagnet in steps of 5–20 mT, up to a field intensity of 70 mT, and then to field intensities of 100, 200 and 400 mT. The 400 mT field was considered sufficient to saturate the ferrimagnetic phases (Cisowski 1981).

A Schonstedt GSD-1 demagnetizer was used for the ARM acquisition studies and for all alternating field demagnetizations. Measurements of remanent magnetization (including ARM and IRM) were done with a 2-G Enterprises Model 760 cryogenic magnetometer.

IRM values were normalized with respect to the saturation IRM (SIRM). Two parameters were used to assess the relative importance of hard (antiferromagnetic) versus soft (ferrimagnetic) phases. These parameters are the *S*-ratio, which is defined as the ratio of IRM acquired in a reverse field of −100 mT to the IRM acquired in a direct field of 400 mT (SIRM), and the remanent coercive force, *Hr*, which is the reverse field necessary to reduce the SIRM to zero. The width of the coercivity spectrum was defined (Dunlop 1986) as the difference between the values of the applied magnetic field at which the IRM was 15 and 85 per cent saturated (H15/H85). Magnetic interactions were studied by determining Wohlfarth's *R*-value (Wohlfarth 1958; Cisowski 1981; Moskowitz *et al.* 1988). This parameter is a measure of the offset between the acquisition and demagnetization curves of the IRM.

EXPERIMENTAL RESULTS

3.1 Transformations of iron in the loess column

The concentration of secondary FeOX (Fe_d) in the 65 samples ranges from 3.0 to 19.5 g kg^{-1} (Fig. 2). The Fe_d in the loess samples corresponds to 15–50 per cent of the maximum concentration that was found in the palaeosols. For the palaeosols, the mean Fe_d and its standard deviation are 14.0 ± 2.6 g kg^{-1}, for the loess these values are 8.9 ± 2.4 g kg^{-1}. The concentration of total iron (Fe_t) in the five loess-palaeosol pairs is given in Table 1. For these samples, Fe_d ranges from 24 per cent of total iron (in a loess) to 31 per cent (in a palaeosol). For each pair, the Fe_t and Fe_d concentrations are slightly greater in the palaeosol than in the loess.

3.2 Magnetic susceptibility of loess and palaeosols

The magnetic susceptibility of the samples ranges from (11 to 324) $\times 10^{-8}$ m^3 kg^{-1}, which is consistent with published results (e.g. Kukla *et al.* 1988). When plotted against Fe_d (Fig. 2), the magnetic susceptibility values fall into two distinct groups: loess and palaeosols. The mean for the palaeosols is $(167 \pm 71) \times 10^{-8}$ m^3 kg^{-1}, while for the loess it is $(44 \pm 16) \times 10^{-8}$ m^3 kg^{-1}. However, the loess samples can also be interpreted as collectively representing the end member from which the palaeosols have developed. Because Fe_d can be taken as a measure of pedogenesis, the data in Fig. 2 support the hypothesis that the enhancement of the magnetic susceptibility is directly related to pedogenesis.

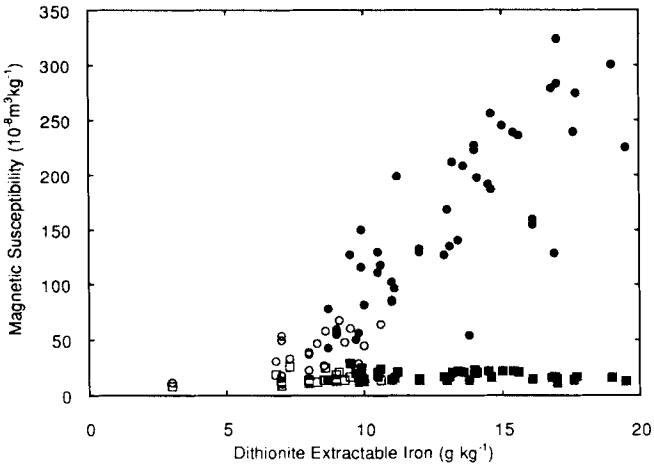

Figure 2. Relationship between magnetic susceptibility (χ) and dithionite extractable iron (Fe_d) for 65 loess (open symbols) and palaeosol (closed symbols) samples. Circles are pre-CBD values, squares are post-CBD values. The close relationship between the pre-CBD values of these two quantities is clearly evident, as is the fact that loess samples with very low magnetic susceptibility still have some extractable iron.

The χ_{FD} values for the 65 samples range from 2.7 to 13.4 per cent, which is also consistent with published results (e.g. Heller *et al.* 1991) (Fig. 3). The mean of the palaeosols is 10.7 ± 1.1 per cent, while that of the loesses is 7.9 ± 2.3 per cent. The parameter χ_{FD} is primarily proportional to the concentration of ferrimagnetic grains near the superparamagnetic/single domain boundary. The magnetic grains produced by pedogenic processes tend to be very fine-grained, so that χ_{FD} tends to increase with pedogenesis until it reaches its maximum observable value which is about 10–12 per cent (Maher 1988). When χ_{FD} is plotted against χ (Fig. 3), the palaeosols exhibit a wide range of χ values but a restricted range of χ_{FD} values, indicating that χ_{FD} is close to or at its maximum value in palaeosols. On the other hand, the loess samples exhibit a narrow range of χ values but a wide range of χ_{FD} values. This implies that there has been some pedogenesis in most of the loess samples (Verosub *et al.* 1993) and that χ_{FD} might be useful in distinguishing the degree of pedogenesis in the loess, as suggested by Liu *et al.* (1993).

After the CBD treatment, the magnetic susceptibilities of all 65 samples became uniformly low, ranging from (9 to 29) $\times 10^{-8}$ m^3 kg^{-1} with a mean of $(17 \pm 4) \times 10^{-8}$ m^3 kg^{-1} (Fig. 2). The post-CBD values of χ_{FD} have a mean of 3.6 ± 1.5 per cent (Fig. 3). There is no significant difference between loess and palaeosol samples. Only two samples had χ_{FD} larger than 6 per cent. In our work with soil chronosequences (e.g. Fine, Singer & Verosub 1992), we have found that soil samples with χ_{FD} values <5 per cent tend to be dominated by multidomain magnetite. We

Table 1. Magnetic and chemical data of palaeosol/loess pairs from Luochuan.

Lithologic Unit*		Depth (m)	χ (10^{-8} m^3 kg^{-1})			χ_{FD} (%)			Fe_d (g/kg)	Fe_t (g/kg)	χ/Fe_d§
			Pre#	Post	Soluble	Pre	Post	Soluble			
Lishi Formation											
S1	(S)	10	199	21	178	11.7	4.7	12.5	11.2	36.2	17.8
L2	(L)	15	31	19	12	6.2	2.1	12.8	6.8	26.4	4.6
S8	(S)	54	130	17	113	10.6	2.8	11.8	10.5	37.3	12.5
L9	(L)	58	27	14	13	6.4	4.5	8.3	8.5	33.5	3.1
S14	(S)	75	116	16	101	10.6	1.1	12.0	9.9	35.1	11.7
L15-LL1	(L)	79	18	13	5	5.2	2.3	12.3	7.0	27.4	2.6
Wucheng Formation											
WL2-SS2	(S)	100	43	14	29	8.4	7.1	9.1	8.7	34.5	5.0
WL2-LL3	(L)	104	39	13	26	8.2	1.4	11.7	8.0	33.4	4.9
WS4-SS3	(S)	126	78	14	64	11.1	2.9	12.8	8.7	35.3	9.0
WL4-LL1	(L)	128	47	12	35	9.8	3.7	11.9	8.3	34.6	5.7
Mean						8.8	3.3	11.5			
Std. Dev.						2.2	1.7	1.5			

* S: palaeosol; L: loess.
# Pre: original untreated sample; Post: after CBD treatment; Soluble: removed by CBD.
§ Units: 10^{-8} m^3 kg^{-1}/(g kg^{-1}).

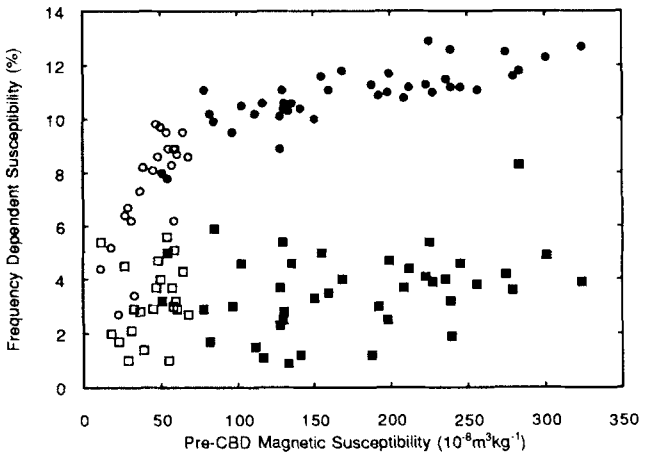

Figure 3. Relationship between frequency dependence of the magnetic susceptibility (χ_{FD}) and pre-CBD magnetic susceptibility (χ) for 65 loess (open symbols) and palaeosol (closed symbols) samples. Circles are pre-CBD values of χ_{FD}, squares are post-CBD values of χ_{FD}. The frequency dependence of the magnetic susceptibility appears to be a useful parameter for assessing the degree of pedogenesis in the loess units but not in the palaeosol units.

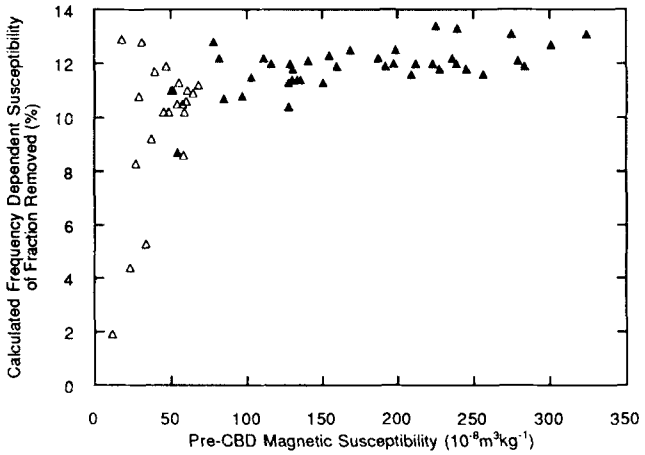

Figure 4. Frequency dependence of the magnetic susceptibility (χ_{FD}) of the CBD-soluble component for 65 loess (open symbols) and palaeosol (closed symbols) samples. The CBD-soluble χ_{FD} is computed from the pre- and post-CBD values of χ at high and low frequencies.

believe that this is probably the case for the loess samples (see below).

Because magnetic susceptibilities are additive, we can calculate χ for the material that was removed by the CBD treatment (soluble χ) by subtracting the post-CBD values from the pre-CBD values. The soluble χ_{FD} can be computed from the soluble χ at high and low frequencies. The mean values of the soluble χ_{FD} were 10.1 ± 2.6 per cent for the loess and 11.7 ± 0.9 per cent for the palaeosols (Fig. 4). Nine samples had soluble χ_{FD} values <8 per cent. These samples were from magnetically less-enhanced loess. The high values of soluble χ_{FD} indicate that the CBD-soluble ferrimagnetic material in almost all of the samples contained a substantial amount of ultrafine-grained superparamagnetic and/or single-domain material. The same conclusion was reached by Banerjee, Hunt & Liu (1993), Liu *et al.* (1993) and Evans & Heller (1994) using other methods.

We also studied the particle-size distribution of the magnetic susceptibility in the palaeosol/loess couplet designated as S1/L2. This couplet immediately underlies the couplet that includes the modern (S0) soil. The magnetic susceptibility of the particle-size fractions of L2 is rather uniform, whereas that in the S1 palaeosol increases with

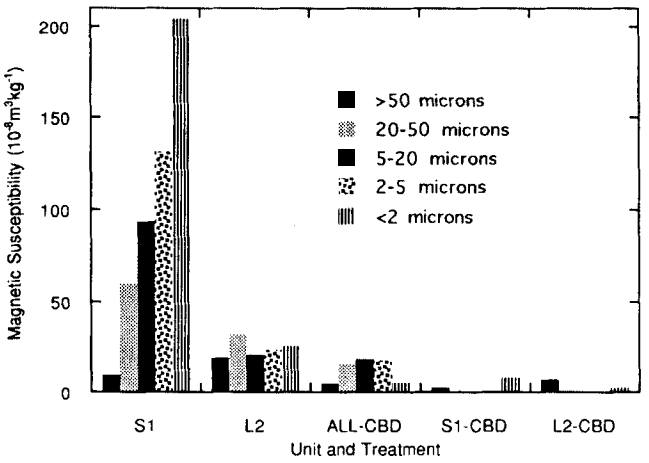

Figure 5. Magnetic susceptibility as a function of particle-size fraction for S1 and L2 palaeosol/loess couplet before CBD treatment and for the sand and clay fractions of those units after CBD treatment. Also shown is the post-CBD magnetic susceptibility as a function of particle-size fraction for a composite sample made of the other four loess/palaeosol couplets from Table 1.

decreasing particle size (Fig. 5). Similar results have been reported previously (Zheng *et al.* 1991; Fine *et al.* 1993). The effect of the CBD treatment on the particle-size distribution of the magnetic susceptibility was studied by treating the sand and clay fractions from the L2 and S1 couplet separately and by combining the particle-size fractions from the other loess/palaeosol couplets in Table 1 into a single suite of samples. All the particle-size fractions have low magnetic susceptibility values after the CBD treatment. These values are comparable with those of the particle-size fractions of the untreated L2 loess.

3.3 Remanence and coercivity parameters

The χ_{ARM} and SIRM of the five loess and palaeosol couplets show a positive linear correlation with the magnetic susceptibility (Fig. 6). The respective ranges of $(0.72–12.2)\times10^{-6}\,m^3\,kg^{-1}$ and $(3.75–12.35)\times10^{-3}\,A\,m^2\,kg^{-1}$ are consistent with published values (e.g. Maher & Thompson 1991). Compared with the least magnetically enhanced loess, the average values of χ, χ_{ARM} and SIRM in the palaeosols are higher by factors of 11, 17 and 3.3, respectively. The differences in these factors represent the inherent dependence of each parameter on the effective ferrimagnetic grain size. Following CBD treatment, χ_{ARM} and SIRM decreased to $(0.26–0.59)\times10^{-6}\,m^3\,kg^{-1}$ and $(1.4–2.1)\times10^{-3}\,A\,m^2\,kg^{-1}$, respectively, regardless of sample type (Fig. 6). This again demonstrates the uniformity of the lithogenic (CBD-resistant) ferrimagnetic component.

Hr and *S*-ratio values from the five couplets are shown in Fig. 7. The higher values of *Hr* and lower values of the *S*-ratio for the palaeosol compared with the loess indicate that the palaeosols are magnetically softer than their loess counterparts, despite the fact that they have higher concentrations of secondary FeOX (Fe_d). After CBD treatment, the coercivity parameters show less variability (Fig. 7), again reflecting the uniformity of the CBD-resistant component.

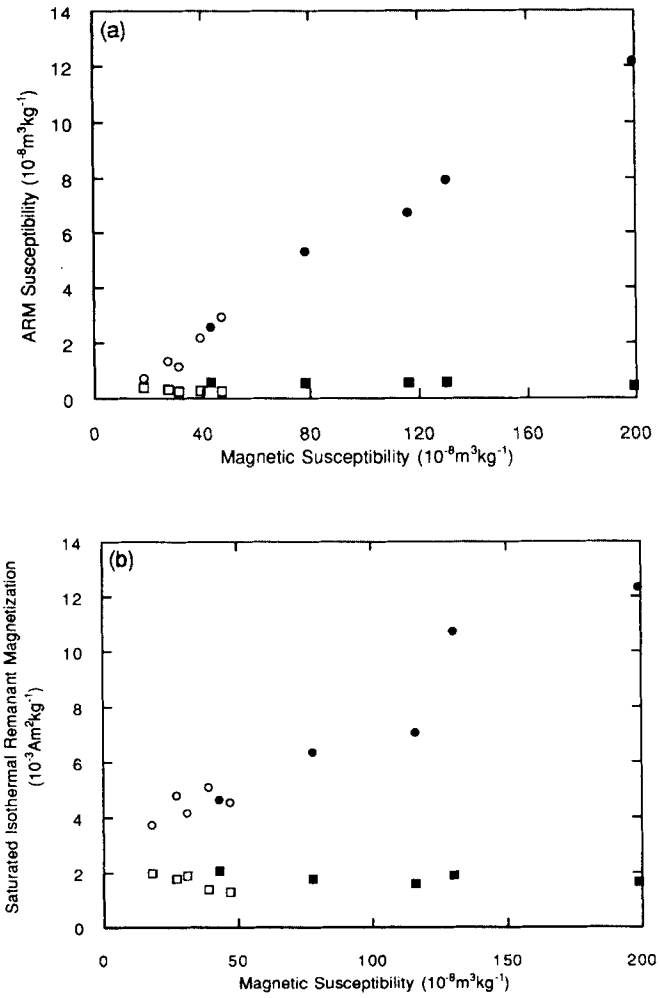

Figure 6. Effect of CBD on magnetic parameters for the five loess/palaeosol couplets in Table 1. Circles are pre-CBD values, squares are post-CBD values; closed symbols are palaeosol samples and open symbols are loess samples. (a) ARM susceptibility (χ_{ARM}) as a function of pre-CBD magnetic susceptibility. (b) Saturated isothermal remanant magnetization (SIRM) as a function of pre-CBD magnetic susceptibility. Both figures show the genetic relationship between the loess and palaeosols as well as the uniformity of the post-CBD component.

The pre-CBD coercivity spectra for the 10 paired samples ranged from 0.034 to 0.146 with a mean of 0.09 ± 0.04 (Fig. 8). We expected that the CBD treatment would narrow the coercivity spectra due to a preferential dissolution of pedogenic (and perhaps other) fine-grained magnetic minerals. The post-CBD spectra ranged from 0.108 to 0.132 with a mean of 0.12 ± 0.01 (Fig. 8). Thus the coercivity spectra became more uniform but remained wide after the CBD treatment.

3.4 Magnetic granulometry of loess and palaeosols

Certain ratios of remanence parameters, in particular χ_{ARM}/χ, χ_{ARM}/SIRM and SIRM/χ, can be used to determine the domain state of ferrimagnetic materials (e.g. Thompson & Oldfield 1986). We determined the pre- and post-CBD values for these three ratios as well as a value for

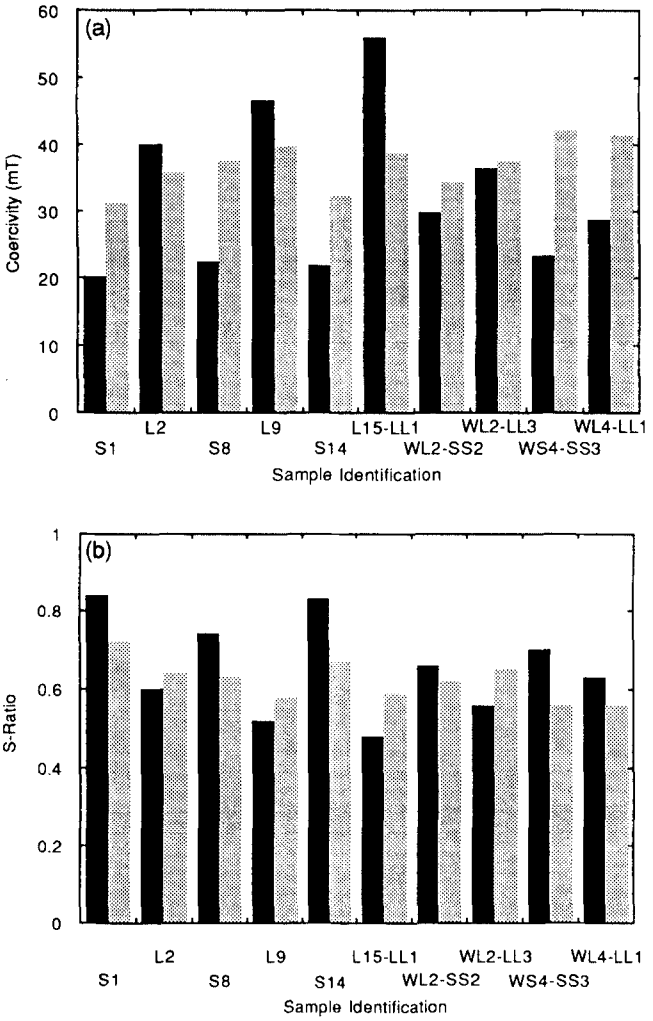

Figure 7. Magnetic hardness of each component of the five loess (L)/palaeosol (S) couplets in Table 1 before and after CBD treatment. Dark bars are pre-CBD, light bars are post-CBD. (a) Coercivity (*Hr*) and (b) *S*-ratio. The figures show that the hardness is controlled primarily by the CBD-resistant component.

the secondary FeOX (Table 2). The latter can be determined because χ, SIRM and χ_{ARM} are not concentration-dependent. Thus, values of these parameters for the CBD-soluble material can be calculated as the difference between the pre- and post-CBD values. The soluble χ, SIRM and χ_{ARM} values can be used to compute the ratios of χ_{ARM}/χ, χ_{ARM}/SIRM, and SIRM/χ for the CBD-soluble component.

The pre-CBD values of χ_{ARM}/χ and χ_{ARM}/SIRM are larger for the palaeosol counterpart within each palaeosol/loess couplet (Table 2). For SIRM/χ the loess values are higher. After CBD treatment, most of the χ_{ARM}/χ and χ_{ARM}/SIRM ratios become lower and more uniform, although the value of these ratios is still higher for a palaeosol than for its loess counterpart. The SIRM/χ ratios also become more uniform, but in this case the change is due to decreases in this ratio for loess samples and increases for palaeosols.

The soluble χ_{ARM}/χ ratios are higher and more uniform than the original values, independent of whether the sample

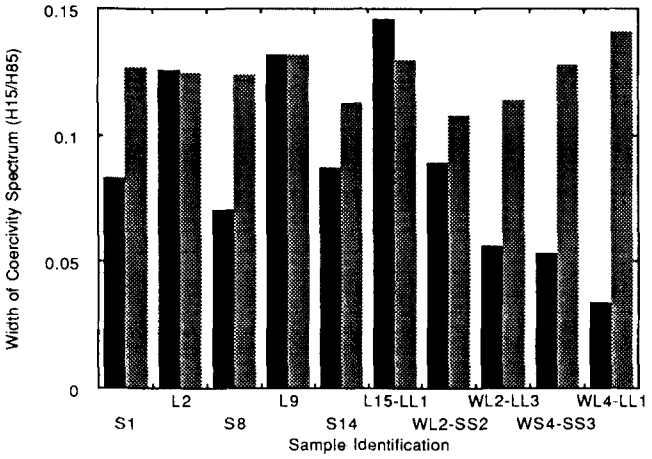

Figure 8. Width of coercivity spectra (H15/H85) of each component of the five loess (L)/palaeosol (S) couplets in Table 1 before and after CBD treatment. H15/H85 is the difference between the values of the applied magnetic field at which the IRM was 15 and 85 per cent saturated. Dark bars are pre-CBD, light bars are post-CBD.

is a loess or a palaeosol (Table 2). The soluble χ_{ARM}/SIRM ratios are higher than the original values, while the soluble SIRM/χ ratios are generally lower than the original values for the palaeosols and higher for the loess (Table 2).

The pre-CBD, post-CBD and soluble values of the χ_{ARM}/χ, χ_{ARM}/SIRM and SIRM/χ ratios are presented in Fig. 9 with respect to their corresponding χ_{FD} values. Only for the χ_{ARM}/χ ratio is there a clear correlation with χ_{FD} (Fig. 9a). For the CBD-treated samples, the low values of χ_{FD} (<5 per cent) and low χ_{ARM}/χ ratios indicate that these samples are dominated by multidomain magnetic grains. At the other end of the spectrum, the high values of χ_{FD} (>9 per cent) and high χ_{ARM}/χ ratios of the more magnetically enhanced palaeosols and of the CBD-soluble secondary FeOX indicate that these samples have magnetic components that are dominated by material near the superparamagnetic/single-domain boundary. The two ratios that contain the SIRM term correlate less well with χ_{FD} (Figs 9b and c). Even the χ_{ARM}/SIRM ratio, which was preferred by Maher (1988) for magnetic granulometry studies, does not show much differentiation for χ_{FD} values up to ≈8 per cent and there is considerable scatter for χ_{FD} values above 11 per cent.

3.5 Magnetic interactions

Wohlfarth's *R*-value is used to determine the importance of internal demagnetizing fields in multidomain grains and interaction fields in single-domain and superparamagnetic grains. For non-interacting, coherently reversing, single-domain ferrimagnetic particles the *R*-value is about 0.5. For the 10 paired samples in this study, the pre-CBD values ranged from 0.39 to 0.47 with a mean of 0.428 ± 0.020 (Fig. 10). After CBD treatment, the range narrowed to 0.416–0.435, but the mean did not change (0.427 ± 0.006). The mean values imply that magnetic interactions are present and the similarity of the pre- and post-CBD values indicates that these interactions are controlled primarily by the CBD-resistant ferrimagnetic material.

Table 2. Magnetic ratios of palaeosol/loess pairs from Luochuan.

Lithologic Unit*		χ_{ARM}/χ			χ_{ARM}/SIRM (10^{-4} A^{-1}m)			SIRM/χ (10^4 A m^{-1})		
		Pre#	Post	Soluble	Pre	Post	Soluble	Pre	Post	Soluble
Lishi Formation										
S1	(S)	6.12	2.16	6.57	9.85	2.74	10.96	0.62	0.79	0.60
L2	(L)	3.67	1.41	7.30	2.77	1.45	3.86	1.33	0.98	1.89
S8	(S)	6.10	3.51	6.48	7.39	3.06	8.33	0.83	1.15	0.78
L9	(L)	5.00	2.36	7.86	2.78	1.84	3.33	1.81	1.29	2.36
S14	(S)	5.79	3.65	6.12	9.53	3.58	11.28	0.61	1.02	0.54
L15-LL1	(L)	3.99	3.05	6.28	1.91	1.95	1.87	2.09	1.57	3.36
Wucheng Formation										
WL2-SS2	(S)	5.94	4.12	6.81	5.54	2.80	7.73	1.07	1.47	0.88
WL2-LL3	(L)	5.58	2.17	7.29	4.28	2.04	5.11	1.30	1.06	1.43
WS4-SS3	(S)	6.84	4.03	7.44	8.38	3.13	10.41	0.82	1.29	0.71
WL4-LL1	(L)	6.22	2.18	7.56	6.47	1.99	8.26	0.96	1.10	0.92
Means and standard deviations										
Mean	(All)	5.52	2.86	6.97	5.89	2.46	7.11	1.14	1.17	0.35
Std. dev.	(All)	0.96	0.88	0.57	2.75	0.66	3.20	0.47	0.22	0.88
Mean	(S)	6.16	3.49	6.68	8.14	3.06	9.74	0.79	1.14	0.70
Std. dev.	(S)	0.36	0.70	0.44	1.57	0.30	1.44	0.17	0.23	0.12
Mean	(L)	4.89	2.23	7.26	0.64	0.85	4.49	1.50	1.20	1.99
Std. dev.	(L)	0.95	0.52	0.53	1.61	0.21	2.16	0.40	0.21	0.84

* S: paleosol; L: loess.
\# Pre: original untreated sample; Post: after CBD treatment; Soluble: removed by CBD.

4 DISCUSSION

The goal of our research has been to identify the different magnetic phases in loess and palaeosols using differential dissolution with CBD. In general, the CBD-resistant magnetic phases are paramagnetic iron-bearing grains in silicate minerals (Mehra & Jackson 1960) and the primary iron oxides magnetite and titanomagnetites (Walker 1983; Fine & Singer 1989; Singer & Fine 1989; Singer *et al.* 1995). In previous studies of soil chronosequences and of this loess column (Fine *et al.* 1989, 1992, 1993; Verosub *et al.* 1993) we have shown that the CBD-resistant component of soils and sediments has low χ_{FD} and χ_{ARM}/χ values, which indicates that multidomain ferrimagnetic phases are predominant. In contrast, the CBD-soluble ferrimagnetic phases usually represent secondary iron oxides (Mehra & Jackson 1960) and/or the weathering products of the primary CBD-resistant iron oxides (e.g. Rebertus & Buol 1985). In well-drained soils, the secondary iron oxides are composed primarily of either antiferromagnetic material (haematite and goethite) or a fine, single-domain and superparamagnetic ferrimagnetic phase with high χ_{FD} and high χ_{ARM}/χ values (Mullins 1977; Maher 1986, 1988; Fine *et al.* 1993). The latter is either maghemite (Fine & Singer 1989; Singer *et al.* 1992) or magnetite (Maher & Taylor 1988) or both (Vodyanitskiy 1981). Ferrihydrite may also be present in small amounts.

In the following sections, we use our data to estimate the partitioning of iron among the various phases and to determine the effects of this partitioning on the mineral magnetic parameters.

4.1 Lithogenic contribution to the magnetic susceptibility signal

In the work reported here, the CBD-resistant iron represents about 70 per cent of total iron (Fe_t) in samples from the loess column. However, the magnetic susceptibility of the CBD-resistant component is low ($17 \pm 4 \times 10^{-8}$ m^3 kg^{-1}), as are its SIRM and χ_{ARM}. Thus most of this iron must be paramagnetic and probably occurs as primary iron-bearing silicate minerals. Based on the concentration of the CBD-resistant iron and on the typical magnetic susceptibility of paramagnetic minerals (Thompson & Oldfield 1986), we can estimate that the maximum contribution to the magnetic susceptibility from the paramagnetic minerals is about 2×10^{-8} m^3 kg^{-1}. The remaining CBD-resistant magnetic susceptibility of about 15×10^{-8} m^3 kg^{-1} must come from lithogenic ferrimagnetic minerals (Maher & Thompson 1992). We estimate the concentration of this phase is $\approx$0.22 g kg^{-1} or about 0.5 per cent of Fe_t, based on a magnetic susceptibility for magnetite of 5×10^{-4} m^3 kg^{-1}, a mole fraction for iron of 0.72, and an Fe_t concentration of 42.6 g kg^{-1}. The Fe_t concentration is estimated from the mean Fe_d/Fe_t ratio of 0.275 for the five couplets and the mean Fe_d concentration of all of the samples.

The lithogenic ferrimagnetic minerals represent a very small fraction of the iron-bearing material, but they have a significant effect on the mineral magnetic properties. For example, as noted above, they appear to control the magnetic interactions and the width of the remanence coercivity spectra. Although the lithogenic ferrimagnetic

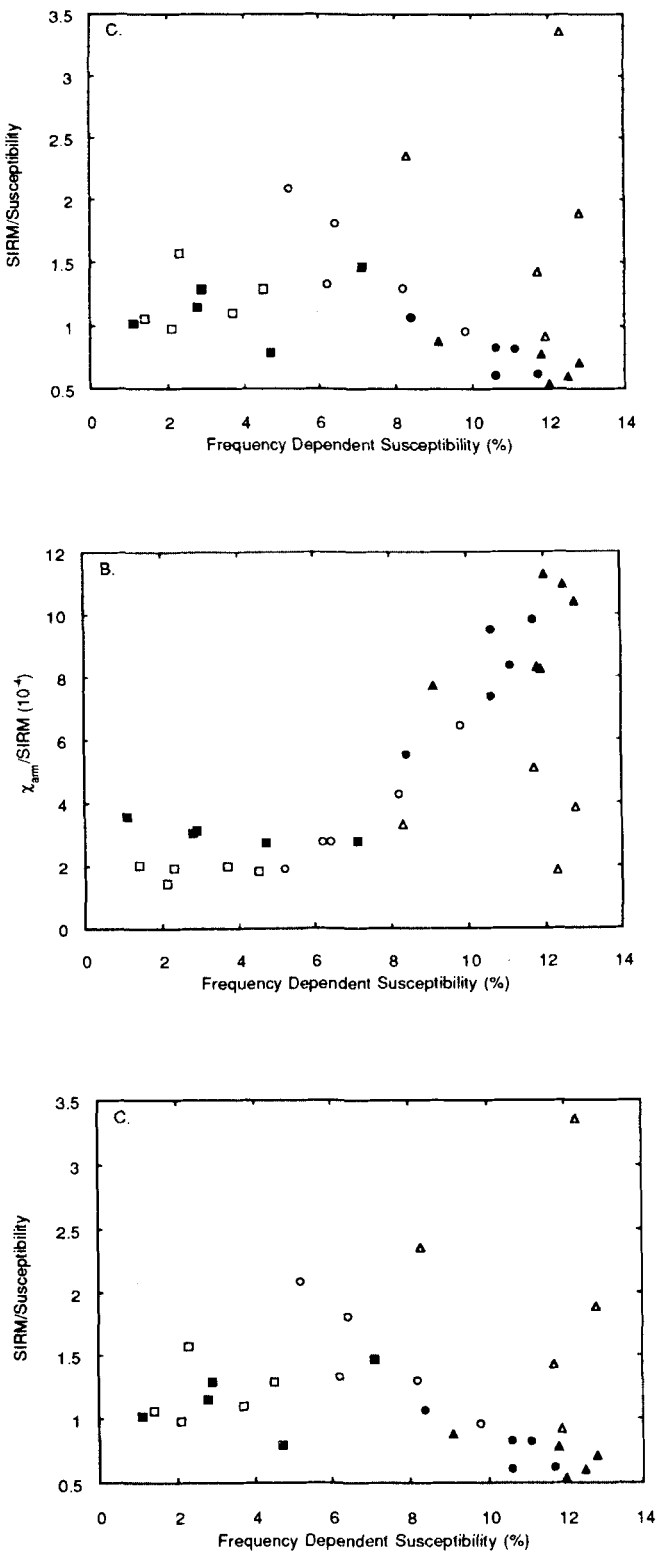

Figure 9. Comparison of magnetic parameters for different components of the five palaeosol/loess couplets. Circles are pre-CBD values, squares are post-CBD values, triangles are values of the CBD-soluble component. Closed symbols are palaeosol samples and open symbols are loess samples. (a) Ratio χ_{ARM}/χ as a function of χ_{FD}. (b) Ratio χ_{ARM}/SIRM as a function of χ_{FD}. (c) Ratio SIRM/χ as a function of χ_{FD}. Only for χ_{ARM}/χ versus χ_{FD} is there a relationship which is independent of the nature of the component.

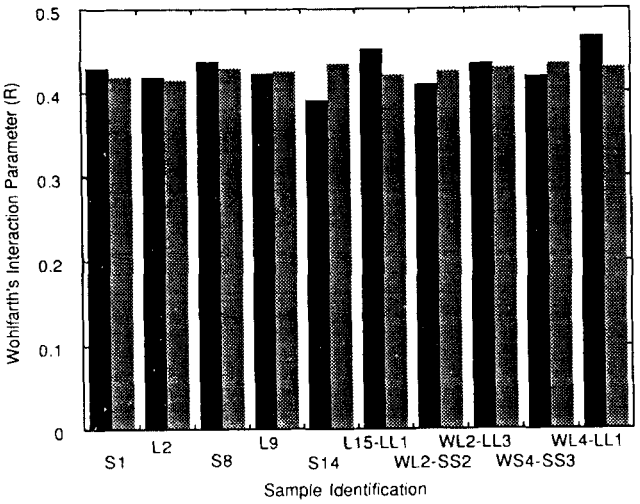

Figure 10. Wohlfarth's interaction parameter (R) for each component of the five palaeosol/loess couplets before and after CBD treatment. Dark bars are pre-CBD, light bars are post-CBD. This parameter is unaffected by the CBD treatment.

minerals are predominantly large multidomain grains, as evidenced by the low values of χ_{FD} and χ_{ARM}/χ, the values of these parameters are not as low as we have found for fresh lithogenic magnetite in beach deposits (~0 per cent and ~0.15, respectively). This result implies that some fraction of the magnetic susceptibility is due to relatively fine-grained material, which agrees with the distribution of the magnetic susceptibility in the different size fractions. Furthermore, the fact that the CBD-resistant clay-size and sand-size particles have nearly equal magnetic susceptibilities (Fig. 5) suggests that the ferrimagnetic grains are associated with or encapsulated in non-magnetic grains that are resistant to the CBD treatment. Otherwise, the fine grains would be preferentially dissolved (Hunt *et al.* 1995).

For the palaeosol/loess couplets, the χ_{ARM}/χ and χ_{ARM}/SIRM ratios of each CBD-treated palaeosol are consistently higher than those of its loess counterpart. We interpret this as indicating that the primary lithogenic ferrimagnetic material has a smaller mean magnetic grain size in the palaeosol than in the loess. If this observation is valid for other palaeosol/loess couplets, it may indicate that the airborne dust reaching our sites during more humid and warm interglacial periods (when soil formation was dominant) had a finer particle-size distribution than the dust that reached these sites during glacial periods (when loess deposition was dominant). However, the effects of these grain-size variations are small in proportion to the CBD-resistant magnetic susceptibility, not to mention the overall magnetic susceptibility. The predominant pattern is that the concentration and the particle-size distribution of the primary lithogenic magnetic material is surprisingly uniform throughout the loess column (at least at the two sites where most of the samples were obtained).

4.2 Pedogenic contribution to the magnetic susceptibility signal

We can estimate the concentration of the CBD-soluble ferrimagnetic and antiferromagnetic components from the Fe_d concentration, the decrease in magnetic susceptibility due to the CBD treatment, and the magnetic susceptibilities

and mole fractions of iron in the ferrimagnetic and antiferromagnetic material. If all of the Fe_d is due to antiferromagnetic material (haematite), the maximum contribution from this component to the magnetic susceptibility is $1.7 \times 10^{-8}\,m^3\,kg^{-1}$, based on the maximum Fe_d ($19.6\,g\,kg^{-1}$), the magnetic susceptibility of haematite ($60 \times 10^{-8}\,m^3\,kg^{-1}$) and the mole fraction of iron (0.7). This figure is one to two orders of magnitude smaller than the observed changes in magnetic susceptibility due to the CBD treatment. Thus, virtually all of the CBD-soluble magnetic susceptibility can be attributed to ferrimagnetic material (maghemite and/or magnetite).

To estimate the concentration of the ferrimagnetic material, we need to know the approximate contribution to the magnetic susceptibility from superparamagnetic grains as well as the ratio of the magnetic susceptibilities of single-domain and superparamagnetic components. Using the result of Banerjee *et al.* (1993), we estimate the superparamagnetic component to be 80 per cent. This value is consistent with the high soluble χ_{FD} values (11 per cent) that we calculated for the secondary FeOX. The magnetic susceptibility of the superparamagnetic particles is approximately twice that of single-domain material (Maher 1988). Based on these estimates, a magnetic susceptibility for maghemite of $5 \times 10^{-4}\,m^3\,kg^{-1}$, and an estimated maximum Fe_t of $63\,g\,kg^{-1}$ (based on Fe_d and the Fe_d/Fe_t ratio), we find that the maximum CBD-soluble magnetic susceptibility of $300 \times 10^{-8}\,m^3\,kg^{-1}$ corresponds to 3.8 per cent of Fe_t. Because Fe_d ranges from 24 to 31 per cent of Fe_t, we conclude that the major component of the secondary FeOX is antiferromagnetic material (haematite) even though this phase does not contribute significantly to the magnetic susceptibility.

Thus about 70 per cent of total iron in the loess column resides in paramagnetic iron-bearing silicate minerals. Almost all of the remainder exists as antiferromagnetic material (haematite). The magnetic susceptibility signal, however, is due primarily to a pedogenic (CBD-soluble) ferrimagnetic phase that comprises up to 3.8 per cent of Fe_t (12 per cent of FeOX) and a lithogenic (CBD-resistant) ferrimagnetic phase that represents about 0.5 per cent of Fe_t. The contribution of the lithogenic phase to the magnetic susceptibility ranges from 60 to 70 per cent in the magnetically less-enhanced loess to a few per cent in the most enhanced palaeosols. This result is consistent with the observation of Hus & Han (1992) that, following magnetic cleaning of samples, the magnetic susceptibility of the L2 loess decreased by 67 per cent while that of the S1 palaeosol decreased by 16 per cent. The differences between our results and those of Hus & Han (1992) can be explained by the fact only the larger lithogenic grains were removed by their method (Fine & Singer 1989).

4.3 Role of pedogenesis

In an earlier paper (Verosub *et al.* 1993) we pointed out that the magnetic susceptibility signal of the loess–palaeosol sequence consisted of at most three components: the CBD-soluble component that represented the difference between the magnetic susceptibility of a palaeosol and its underlying loess, the CBD-soluble component that was common to both the palaeosol and its underlying loess, and the residual, CBD-resistant component. Because the second component was CBD-soluble, we concluded that it was related to pedogenesis, or more broadly, weathering. We suggested that this weathering might have taken place in the source area of the loess prior to its removal and deposition on the loess plateau, or it might have been the product of weak *in situ* pedogenesis after deposition. We believe that our new data support the second hypothesis. In the loess, which presumably most closely resembles material from the source area, the Fe_d was high, but the magnetic susceptibility was very low. Furthermore, the magnetic susceptibility was linearly correlated to Fe_d, indicating gradual enrichment of the secondary FeOX as a result of the formation of pedogenic iron phases. For zero magnetic susceptibility, the calculated Fe_d was $6.4\,g\,kg^{-1}$ (Fig. 2). We interpret this result as indicating that the weathering environment in the source area of the loess was conducive to the transformation of primary iron into secondary iron oxides, but not to the formation of ferrimagnetic material. Thus, most of the CBD-soluble ferrimagnetic material should be attributed to pedogenesis in the loess/palaeosol sequence. This conclusion is consistent with our previous conclusion that loess deposition and pedogenesis were competing processes at all times, and the presence of a palaeosol simply indicates that the latter process was predominant (Verosub *et al.* 1993; Fine *et al.* 1993).

The properties of the pedogenic ferrimagnetic material can be studied by comparing the magnetic properties of untreated samples with those of the soluble component, as described above. Both the enhancement of the magnetic susceptibility and the enrichment of secondary FeOX indicate that the authigenic ferrimagnetic material consists predominantly of superparamagnetic grains. For example, the χ_{FD} of untreated samples increases steeply even with small increases in χ (Fig. 3), indicating that changes in the amount of superparamagnetic material are large enough to affect the overall magnetic properties. The effect is even more dramatic when we consider the magnetic properties of the secondary FeOX itself (the soluble component). The soluble χ_{FD} values for all but nine of the samples ranged from 8 to 13 per cent (Fig. 3). The other nine samples were from non-enhanced loesses, with CBD-soluble magnetic susceptibilities of less than $15 \times 10^{-8}\,m^3\,kg^{-1}$. The high χ_{FD} values imply a significant superparamagnetic contribution. Increases in the values of the χ_{ARM}/χ and χ_{ARM}/SIRM and a gradual decrease of the magnetic coercivity ('softening') with increasing Fe_d or magnetic susceptibility also indicate high proportions of superparamagnetic material. Had the pedogenic ferrimagnetic material been dominated by single-domain grains instead of superparamagnetic grains, there would have been a substantial increase in the magnetic coercivity ('hardening') of the samples. Using other approaches, Banerjee *et al.* (1993), Liu *et al.* (1993) and Evans & Heller (1994) also concluded that the primary ferrimagnetic product of pedogenesis was superparamagnetic grains.

4.4 Understanding the magnetic record

Based on the CBD treatment and on the calculated magnetic properties of the secondary FeOX (Fig. 9), we conclude that χ_{ARM}/χ provides a better representation of the grain-size distribution of the ferrimagnetic material than either χ_{ARM}/SIRM or SIRM/χ. We believe that the reason

for this is that the latter two ratios are affected by antiferromagnetic material even at the 0.4 T maximum field that we applied. In fact, SIRM should not be used for magnetic granulometry in any samples that have a mixed magnetic mineralogy consisting of ferrimagnetic material (magnetite or maghemite) and a significant amount of anti-ferromagnetic material (haematite). The close correlation between χ_{FD} and χ_{ARM}/χ (Fig. 9a) suggests that these magnetic parameters are sensitive to magnetic particles in the same size range, perhaps the 16–23 nm range suggested by Maher (1988).

This particular study does not resolve the question of the exact mineralogy of the ferrimagnetic material in the loess column, although Banerjee *et al.* (1993) have pointed out that understanding the mineralogy may be less important than understanding its origin, content and distribution. Since workers strongly favour magnetite as the main pedogenic mineral, either chemically precipitated (Maher & Thompson 1991; Maher & Taylor 1988) or biogenic (Maher & Thompson 1992; Evans & Heller 1994). Using measurements of magnetic properties, X-ray diffraction data and Mossbauer spectra, we have shown that maghemite is the main pedogenic phase in soil chronosequences in California (Fine & Singer 1989; Singer *et al.* 1995). We believe that maghemite also plays an important role in the ferrimagnetic enhancement of the Chinese loess/palaeosol sequence, and recent mineral magnetic studies at low and high temperatures appear to support this point of view (Verosub *et al.* 1994; Eyre & Shaw 1994).

Our conclusions about the nature of the magnetic susceptibility signal and about the importance of pedogenesis are based on CBD treatment of samples from Luochuan and Liujiapo (Fig. 1). This raises the possibility that our results might reflect circumstances that are particular to these two sites. We believe that this is unlikely because other researchers using different techniques and working at various sites have also concluded that the enhancement of the magnetic susceptibility signal is due to ultra-fine grained ferrimagnetic material produced by pedogenesis (Heller *et al.* 1991; Hus & Han 1992; Banerjee *et al.* 1993; Liu *et al.* 1993; Evans & Heller 1994). Only at Xifeng has it been suggested that depositional rather than pedogenic processes were important in the enhancement of the magnetic susceptibility (Guo *et al.* 1993); however, another group came to the opposite conclusion about this same site (Liu *et al.* 1993).

The controversy concerning Xifeng underscores the importance of using a variety of methods to obtain a more complete understanding of the nature of the magnetic signal in the Chinese loess plateau or the underlying palaeoclimate record that produced it. Recent studies have used mineral magnetic methods, petrographic methods and geochemical methods to address this problem (e.g. Maher & Thompson 1992; Banerjee *et al.* 1993; Liu *et al.* 1993; Guo *et al.* 1993; Beer *et al.* 1993; Evans & Heller 1994). In this paper we have shown how additional information can be obtained by combining mineral magnetic methods with a technique commonly used in soil science.

5 CONCLUSIONS

Our work on samples primarily from Luochuan and Liujiapo shows that the same magnetic phases are present throughout the loess column, but because of pedogenesis, the proportions of the constituents are different in loess and palaeosol units. The four iron phases that we observe follow.

(1) Paramagnetic iron associated with silicate minerals. This iron constitutes about 70 per cent of total iron (Fe_t).

(2) Antiferromagnetic material which constitutes most of the secondary iron oxides and oxyhyroxides produced by weathering and pedogenesis. The contribution of this material to Fe_t ranges from 24 per cent of Fe_t in loess to 31 per cent in palaeosols. In terms of total concentration, this phase is twice as important in the palaeosols as in the loess.

(3) Lithogenic multidomain magnetite and titanomagnetites which are present in low, nearly uniform concentrations ($\simeq$0.5 per cent of Fe_t) and particle sizes in all the samples. The mean magnetic grain size (inferred from ratios of magnetic parameters) is somewhat finer in the palaeosols than it is in their loess counterparts.

(4) Pedogenic ferrimagnetic material which constitutes up to 3.8 per cent of Fe_t and consists predominantly of superparamagnetic grains of either magnetite or maghemite. The accumulation of this material is directly related to the degree of pedogenesis, and it is this material that generates the magnetic susceptibility enhancement in the loess plateau.

The relative concentrations of the four magnetic phases control the magnetic behaviour of the samples. The accumulation of the pedogenic superparamagnetic phase results in a lower magnetic coercivity in the palaeosols, despite a coincident increase in the concentration of higher coercivity antiferromagnetic material. However, the width of the coercivity spectra and the magnetic interactions in all the samples are controlled by the lithogenic multidomain magnetite and titanomagnetite, despite their small contribution to the overall Fe_t.

This work confirms our earlier conclusion and that of others that the palaeoclimate record of the loess/palaeosol sequence is primarily a record of pedogenesis (Hus & Han 1992; Banerjee *et al.* 1993; Verosub *et al.* 1993; Liu *et al.* 1993; Evans & Heller 1994). It also demonstrates that the CBD technique can provide a means of studying the partitioning of iron into various magnetic and non-magnetic phases and a means of characterizing the magnetic properties of the pedogenic fraction of that iron.

ACKNOWLEDGMENTS

This work was supported by NSF grants EAR 88-03926 and EAR 91-17790.

REFERENCES

Banerjee, S.K., Hunt, C.P. & Liu, X.M., 1993. Separation of local signals from the regional paleomonsoon record of the Chinese loess plateau: A rock-magnetic approach, *Geophys. Res. Lett.*, **20,** 843–846.

Beer, J., Shen, C.D., Heller, F., Liu, T.S., Bonani, G., Dittrich, B., Suter, M. & Kubik, P., 1993. ^{10}Be and magnetic susceptibility in Chinese loess, *Geophys. Res. Lett.*, **20,** 57–60.

Cisowski, S., 1981. Interacting vs. non-interacting single domain behavior in natural and synthetic samples, *Phys. Earth planet. Inter.*, **26,** 56–62.

Dunlop, D.J., 1986. Coercive forces and coercivity spectra of submicron magnetites, *Earth planet. Sci. Lett.*, **78,** 288–295.

Evans, T.E. & Heller, F., 1994. Magnetic enhancement and palaeoclimate: study of a loess/paleosol couplet across the Loess Plateau of China, *Geophys. J. Int.*, **117,** 257–264.

Eyre, J.K. & Shaw, J., 1994. Magnetic enhancement of Chinese loess—the role of γFe_2O_3, *Geophys. J. Int.*, **117,** 265–271.

Fine, P. & Singer, M.J., 1989. Contribution of ferrimagnetic minerals to oxalate- and dithionite-extractable iron, *Soil Sci. Soc. Am. J.*, **53,** 191–196.

Fine, P., Singer, M.J., La Ven, R., Verosub, K.L. & Southard, R.J., 1989. Role of pedogenesis in distribution of magnetic susceptibility in two California chronosequences, *Geoderma*, **44,** 287–306.

Fine, P., Singer, M.J. & Verosub, K.L., 1992. The use of magnetic-susceptibility in assessing soil uniformity in chronosequence studies, *Soil Sci. Soc. Am. J.*, **56,** 1195–1199.

Fine, P., Singer, M.J. & Verosub, K.L., 1993. New evidence for the origin of ferrimagnetic minerals in the loess column from China, *Soil Sci. Soc. Am. J.*, **57,** 1537–1542.

Guo, Z.T., Fedoroff, N., An, Z.S. & Liu, T.S., 1993. Interglacial dustfall and origin of iron oxide-hydroxides in the paleosols of Xifeng loess section, China, *Scient. Geol. Sinica*, **2,** 91–100.

Heller, F. & Liu, T.S., 1984. Magnetism of Chinese loess deposits, *Geophys. J. R. astr. Soc.*, **77,** 125–141.

Heller, F. & Liu, T.S., 1986. Palaeoclimatic and sedimentary history from magnetic susceptibility of loess in China, *Geophys. Res. Lett.*, **13,** 1169–1172.

Heller, F., Liu, X.M., Liu, T.S. & Xu, T.C., 1991. Magnetic susceptibility of loess in China, *Earth planet. Sci. Lett.*, **103,** 301–310.

Hunt, C.P., Singer, M.J., Kletetschka, G., TenPas, J. & Verosub, K.L., 1995. Effect of citrate-bicarbonate-dithionite treatment on fine-grained magnetite and maghemite, *Earth planet. Sci. Lett.*, **130,** 87–94.

Hus, J.J. & Han, J., 1992. The contribution of loess magnetism to the retrieval of past global changes—some problems, *Phys. Earth planet. Inter.*, **70,** 154–168.

Kukla, G. & An, Z.S., 1989. Loess stratigraphy in central China, *Palaeogeog. Palaeoclim. Palaeoecol.*, **72,** 203–225.

Kukla, G., Heller, F., Liu, X.M., Xu, T.C., Liu, T.S. & An, Z.S., 1988. Pleistocene climates in China dated by magnetic susceptibility, *Geology*, **16,** 811–814.

Liu, X.M., Shaw, J., Liu, T.S., Heller, F. & Yuan, B.Y., 1992. Magnetic mineralogy of Chinese loess and its significance, *Geophys. J. Int.*, **108,** 301–308.

Liu, X.M., Shaw, J., Liu, T.S. & Heller, F., 1993. Magnetic susceptibility of the Chinese loess-paleosol sequence: environmental change and pedogenesis, *J. geol. Soc. Lond.*, **150,** 583–588.

Maher, B.A., 1986. Characterization of soils by mineral magnetic measurements, *Phys. Earth planet. Inter.*, **42,** 76–92.

Maher, B.A., 1988. Magnetic properties of some synthetic sub-micron magnetites, *Geophys. J.*, **94,** 83–96.

Maher, B.A. & Taylor, R.G., 1988. Formation of ultrafine-grained magnetite in soil, *Nature*, **336,** 368–370.

Maher, B.A. & Thompson, R., 1991. Mineral magnetic record of Chinese loess and Paleosols, *Geology*, **19,** 3–6.

Maher, B.A. & Thompson, R., 1992. Paleoclimatic significance of the mineral magnetic record of the Chinese loess and paleosols, *Quaternary Research*, **37,** 155–170.

Mehra, O.P. & Jackson, M.L., 1960. Iron oxide removal from soils and clays by dithionite-citrate system buffered with soidum bicarbonate, *Clays and Clay Min.*, **5,** 317–327.

Moskowitz, B.M., Frankel, R.B., Flanders, P.J., Blakemore, R.P. & Schwartz, B.B., 1988. Magnetic properties of magnetotactic bacteria. *J. Magn. magn. Mat.*, **73,** 273–288.

Mullins, C.E., 1977. Magnetic susceptibility of the soil and its significance in soil science—A review, *J. Soil Sci.*, **28,** 223–246.

Rebertus, R.A. & Buol, S.W., 1985. Iron distribution in a developmental sequence of soils from mica gneiss and schist, *Soil Sci. Soc. Am. J.*, **49,** 713–720.

Singer, M.J. & Janitzky, P., eds, 1986. Field and laboratory procedures used in a soil chronosequence study, *U.S. Geol. Surv. Bull.* **1648.**

Singer, M.J. & Fine, P., 1989. Pedogenic factors affecting magnetic susceptibility of northern California soils, *Soil Sci. Soc. Am. J.*, **53,** 1119–1127.

Singer, M.J., Fine, P., Verosub, K.L. & Chadwick, O.A., 1992. Time dependence of magnetic susceptibility of soil chronosequences on the California coast, *Quaternary Research*, **37,** 323–332.

Singer, M.J., Bowen, L.H., Verosub, K.L., Fine, P. & TenPas, J., 1995. Mossbauer spectroscopic evidence for citrate-bicarbonate-dithionite extraction of maghemite from soils, *Clays and Clay Min.*, in press.

Thompson, R. & Oldfield, F., 1986. *Environmental Magnetism*, Allen & Unwin, London.

Verosub, K.L., Fine, P., Singer, M.J. & TenPas, J., 1993. Pedogenesis and paleoclimate: Interpretation of the magnetic susceptibility record of Chinese loess-paleosol sequences, *Geology*, **21,** 1011–1014.

Verosub, K.L., Fine, P., Singer, M.J. & TenPas, J., 1994. Reply to comments on "Pedogenesis and paleoclimate: Interpretation of the magnetic susceptibility record of Chinese loess-paleosol sequences," *Geology*, **22,** 859–860.

Vodyanitskiy, Y.N., 1981. Formation of ferromagnetics in sod-podzolic soil, *Soviet Soil Sci.*, **12,** 89–100.

Walker, A.L., 1983. The effects of magnetite on oxalate- and dithionite-extractable iron, *Soil Sci. Soc. Am. J.*, **47,** 1022–1026.

Wohlfarth, E.P., 1958. Relations between different methods of acquisition of the remanent magnetization of ferromagnetic particles, *J. Appl. Phys.*, **29,** 595–596.

Zheng, H., Oldfield, F., Yu, L., Shaw, J. & An, Z., 1991. The magnetic properties of particle-sized samples from the Luo Chuan loess section: evidence for pedogenesis, *Phys. Earth planet. Inter.*, **68,** 250–258.

Zhou, L.P., Oldfield, F., Wintle, A.G., Robinson, S.G. & Wang, J.T., 1990. Partly pedogenic origin of magnetic variations in Chinese loess, *Nature*, **346,** 737–739.

APPENDIX A: NOTATION

FeOX	Secondary iron oxides
CBD	Citrate-dithionite-bicarbonate (extraction procedure)
Fe_d	Concentration of CBD-soluble iron
Fe_t	Total iron concentration
χ	Magnetic susceptibility
χ_{FD}	Frequency dependence of magnetic susceptibility
ARM	Anhysteretic remanent magnetization
χ_{ARM}	ARM susceptibility
IRM	Isothermal remanent magnetization
SIRM	Saturation isothermal remanent magnetization
Hr	Coercivity of remanence
S-ratio	IRM acquired in field of −100 mT/IRM acquired in field of 400 mT
H15/H85	Width of the coercivity spectrum
R value	Wohlfarth's magnetic interaction parameter.